A Preliminary Assessment of the RANGE Mission's Orbit Determination Capabilities

AE 8900 MS Special Problems Report
Space Systems Design Lab (SSDL)
Guggenheim School of Aerospace Engineering
Georgia Institute of Technology
Atlanta, GA

Author:
Austin W. Claybrook

Advisor:
Prof. Brian C. Gunter

August 03, 2018

Abstract

The primary mission object of the Ranging And Nanosatellite Guidance Experiment (RANGE) is the demonstration of precision position determination on the nanosatellite platform expected to launch in late 2018. RANGE consists of two 1.5U CubeSats each with a high precision GNSS receiver. The GNSS receiver on each satellite receives GPS pseudoranges and phases in the civilian L1 and L2 frequencies, which will be used for precision orbit determination. The receiver clocks are supplemented by high precision atomic clocks to reduce timing uncertainties. The satellites also host a near proximity laser ranging system to reduce relative in-track orbit uncertainties. A preliminary examination of the RANGE mission's orbit capabilities suggests a 3σ position uncertainty of less than 10 cm in the radial, intrack and crosstrack direction when taking GPS measurement once per minute. During select times of higher frequency 1 second logging, the 3σ position uncertainty in the radial, intrack and cross track directions may be driven down to the 2.5 cm, 1 cm and 1.5 cm level, respectively. Hardware in the loop simulations with a GPS signal generator have verified the performance of the CubeSat hardware against the hardware spec sheets and show increased clock stability when the atomic clock is used. Once the RANGE missios has launched, ground based laser ranging measurements provided by the NRL and ILRS will be used to independantly validate the post processed precision orbit determination solutions of the RANGE mission.

Nomenclature

$1PPS$	1 pulse per second
ADR	Accumulated Doppler range
$COTS$	Commercial off the shelf
$CSAC$	Chip Scale Atomic Clock
EKF	Extended Kalman filter
$GNSS$	Global Navigation Satellite System
GPS	The Global Positioning System
IGS	International GNSS Service
$ILRS$	International Laser Ranging Service
$L1$	GPS carrier frequency at 1575.42 MHz
$L2$	GPS carrier frequency at 1227.60 MHz
LEO	Low Earth orbit
NRL	U.S. Naval Research Lab
$ODTK$	Orbit Determination Tool Kit
$RANGE$	Ranging And Nanosatellite Guidance Experiment
RF	Radio frequency
$RINEX$	Receiver Independent Exchange Format
RMS	Root mean square
SLR	Satellite laser ranging

1 Introduction

As of August 2018, the prime example of precise orbit determination with a CubeSat formation is the Canadian Advanced Nanospace eXperiment -4&5 (CanX -4&5). CanX -4&5 are a pair of 1U CubeSats demonstrating formation flight, developed by the University of Toronto, Institute for Aerospace Studies/Space Flight Laboratory [1]. Launched in June 2014, the CubeSats demonstrated formation flight with sub-meter level position determination and control using a Novatel GPS receiver and an relative motion Extended Kalman Filter (EKF) and smoother measurement processing scheme. The single point GPS navigation solutions were generally accurate to within 10 m, but had occasional with spikes reducing accuracy to 30 m. The radial position residuals were on the order of 10 m, while the in-track ad cross-track residuals were generally less than 10 m. After applying the on board relative EKF algorithm, the GPS pseduorange and carrier phase measurements residuals generally had a zero mean Gaussian distribution. The pseudorange residuals were generally less than 1 m and the carrier phases were generally accurate to less than 0.01 m. The exact orbit determination accuracies were not explicitly stated, but given the 3D-RMS position control error of of approximately 0.5 m and GPS residuals accuracies, the relative orbit determination solution is likely on the order of centimeters.

Another successful demonstration of precise orbit determination for small satellites came from the the FORMOSAT-3/COSMIC mission, a 6 satellite joint mission by Taiwan and the US which was launched in April 2006. The satellites were able to achieve post-processed orbit determination solutions to within 1-3 cm by using zero-difference carrier phase measurements from two GPS antennas on each satellite, albeit the satellites were notably larger than CubeSats with a mass of 62 kg. The software used by for the COSMIC mission was Bernese Version 5.0, which allows for reduced dynamics and kinematic orbit determination. For the reduced dynamic approach, the estimated parameters included the six elements of a Cartesian state vector, nine solar radiation coefficients, and three pseudo-stochastic pulses every 6 min in the radial, in-track and cross-track directions [2]. As shown by Švehla and Rothacher [3], the pseudo-stochastic pulses absorb mismodeled LEO dynamics to a allow for 1-3 cm orbit solutions. The dynamics used consisted of an Earth gravity model, solid, ocean and pole tides, and third body planetary ephemerides. The reduced dynamic approach and the kinematic orbit determination approach yielded similar results to the 2-3 cm level. These orbit determination levels are derived from two 30 hour data arcs, which partially overlapped. Orbit determination was performed using overlaps of both 5 and 6 hours, and both yielded similar orbit determination accuracies. Data collection was taken at 5 second and 30 second increments, both yielded similar results. Two sources of independent analysis conducting by the University Corporation for Atmospheric Research and the Wuhan University were able to match orbit solutions of the COSMIC mission to within 10 cm RMS, with the largest difference suspected to be caused by a mis-match in dynamics and different GPS ephemerides.

The primary motivation for this work and one of the primary mission objects for the RANGE mission is to demonstrate centimeter level post processed orbit solutions capability for nanosatellites. Nanosatellite popularity is rapidly growing within the industry with key benefits over larger scale more conventional spacecraft buses. Many payloads which previously required larger multimillion dollar satellites to power and operate, have now been miniaturized to have a much smaller form factors with similar capabilities. Nanosatellites also offer advantages with lower mission life development times, easier satellite constellation replacements and much lower costs in general, making them more widely accessible to small scale businesses and universities [4]. A distributed formation of nanosatellites, can produce the same mission capability of larger singular satellites with the addition benefits of fault tolerance, reconfigurability, and upgradability. However, formation flight comes with the challenges of precision orbit determination, attitude determination and control, and tight station keeping. Improvement orbit determination accuracies are directly applicable to enhancing the feasibility of many planned formation flight missions. Currently, over 30 formation flight missions are in concept, development, have a launch date, or have been launched [5]. Funding for these missions is coming from large organizations such as NASA, the National Science Foundation, the Department of Defense, the European Space Agency, the Canadian Space Agency, the Chinese Academy of Sciences, universities and private companies. The mission objects of these nanaosatellies vary from Earth science, astronomy ans astrophysics, planetary studies, heliophysics and technology demonstrations.

RANGE aims to improve upon the state of the art orbit determination accuracies by demonstrating centimeter level absolute position uncertainties capabilities on a nanosatellite platform using commercial off the shelf (COTS) components. Currently, the state of the art orbit determination for absolute positioning, relative positioning and relative position control are 2-5 m, 2-5 cm and 1 m rms, respectively, as demonstrated by the CanX-4&5 mission.

2 Methods

To achieve precision orbit determination below the meter level the CubeSat hardware must be capable of the producing the required measurement accuracies. The following sections outline the RANGE mission hardware selection and capabilities, the measurements types, the orbit determination scheme, and measurement accuracy validation methods from a hardware in the loop simulation.

2.1 Hardware

2.1.1 Novatel OEM6 628 GNSS Receiver

The primary measurements used for orbit determination come from a GNSS receiver on board each satellite. The specific GNSS receivers used are the Novatel OEM6 628 boards, as shown in figure 1. The driving factors for the choice of these receivers are the GPS single measurement accuracies, the support for an external oscillator, and the removal of the altitude and velocity limits by the manufacturer. The horizontal accuracy of a single point positioning solution for a stationary receiver using L1 and L2 is less than 2 meters [6]. From hardware in the loop testing of the Novatel boards, the predicted on orbit single point positioning is often within 10 meters of the simulated true position, discussed in more detail in subsection 2.4. Meter level position determination without any post-processing is better than many commercial satellites. The meter level absolute position accuracy from the single point positioning solution provides the accurate initial state and covariance estimates needed to drive the post-processed orbit solutions down to centimeter level. The particular OEM6 628 model supports the use of an external atomic oscillator to discipline the receiver clock, making the OEM6 628 model the only candidate in the OEM6 series. Lastly, Novatel agreed to remove the altitude and velocity restrictions for a government approved research mission. The removal of the velocity restrictions is a critical requirement and distinguisher from other COTS GNSS receivers. These factors make the Novatel OEM6 boards a excellent candidates for readily available COTS hardware to be used for precision orbit determination.

The Novatel OEM6 628 boards support GPS, GLONAS, Galileo, BeiDou, QZSS and SBAS measurements. For the RANGE mission, only GPS is used. Up to 120 channels can be tracked at once, allowing for any GPS satellites in view to be tracked. The GPS signals able to be tracked include the L1, L2, and L5 frequencies. Once in orbit, the pseudorange and carrier phase for the civilian L1 and L2 frequencies will be collected for each GPS satellite signal received. The GPS data is collected by the rangecmp2 log, which is a compressed format allowing for more data collection, which will later be downlinked, extracted and post processed on the ground. The log contains a base pseudorange, carrier phase, an Doppler shift measurement for each satellite, which is then combined with a frequency specific signal block to yield the received signal. The log also contains estimated measurement uncertainties and a clock steering status which are useful for data filtering. The GNSS antenna used in pair with the Novatel receiver is an Antcomm GPS antenna. The Antcomm GPS antenna is capable of receiving L1 and L2 GPS frequencies. Thus the L5 frequency will not be used.

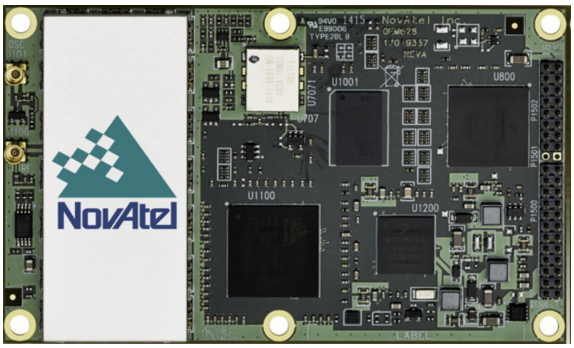

Figure 1: Novatel OEM6 628 receiver board

2.1.2 Atomic Clock

The external oscillator used to discipline the Novatel is the 10MHz Chip Scale Atomic Clock (CSAC) created by Jackson Labs, as shown in figure 2. The 10MHz signal provided by the CSAC is used by the GPS receiver to reduce the GPS receivers clock drift and reduce the timing uncertainty. The CSAC's clock is kept from drifting by receiving a 1PPS from the Novatel and comparing the signal to an internally generated 1PPS signal. In this way, the CSAC is kept within an average phase lock of 0.3 nanoseconds with the GPS receiver and the pair are kept within 10 nanoseconds of UTCG [7]. Thus the long term drift of the CSAC is removed when connected to an active GPS receiver. If GPS signal is lost, the CSAC keeps the Novatel clock steady, with minimal drift will trying to reacquire signal.

Figure 2: CSAC by Jackson Labs [7]

After a day of GPS signal lock the square root of the Allan Variance, $\sigma(\tau)$, approaches deviations on the order of $1e^{-12}$ to $1e^{-13}$ seconds. When the CSAC is not connected to a GPS signal, the stability of the free running CSAC is on the order of $1e^{-11}$ seconds, as shown in 3. The time deviation of the CSAC-Novatel pair is 4 to 5 orders of magnitudes better than the $2e^{-8}$ seconds accuracy of the Novatel on its own. The improved stability of the Novatel clock will serve the three primary functions, reducing timing uncertainty for received GPS pseudoranges, better characterization of the time bias and reduced uncertainty when timing laser ranging pulses between the CubeSats during periods of near-proximity operations.

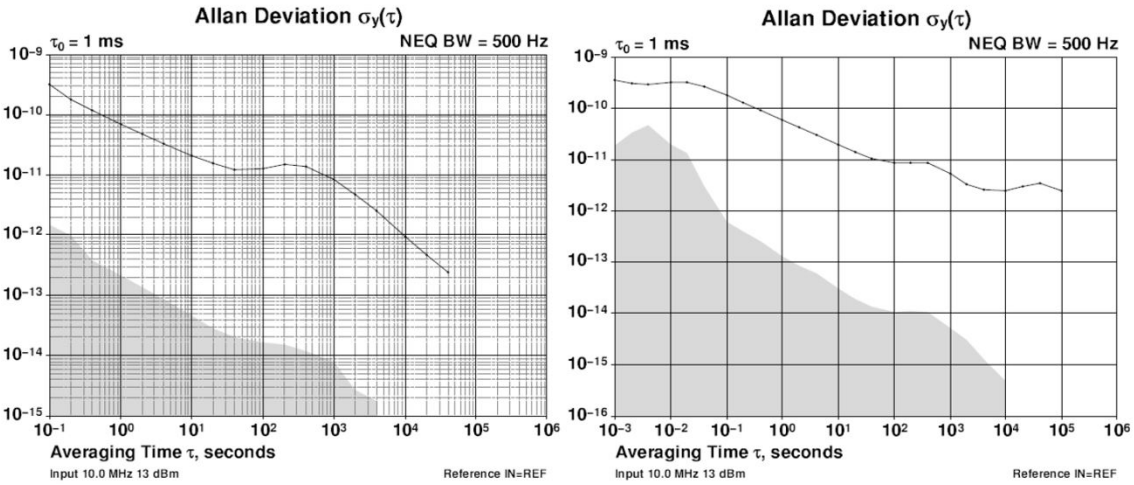

Figure 3: CSAC Allan Deviation over time a) with a GPS signal lock b) without a GPS signal lock [7]

2.1.3 Laser Ranging System

The laser ranger used is the Voxel Laser Range Finder, which is capable of 150 mm single pulse accuracies and 50 mm accuracies with multi-pulse detection [8]. The laser rangers have a ranging and detection capabilities out to 3 km for a single pulse and 5 km for a multi-pulse signal. The laser rangers act as an independent measurement source to supplement the GPS measurements, which will help constrain the CubeSat relative positioning during near proximity operations.

2.2 Measurements

2.2.1 GPS Measurements

GPS pseudorange and carrier phase are observed in the L1 and L2 frequencies from the Novatel OEM6 628 boards. The GPS signal measurements can be used to generate a single point position estimate for the spacecraft. When at least 4 GPS satellite pseudorange measurements are received by the Novatel, the receiver can estimate the CubeSat's position and clock bias. A state vector, consisting of three unknown position components and one unknown time component can be estimated with four known GPS ranges.

$$\mathbf{x} = [x, y, z, \delta t \ c]^T \tag{1}$$

Four GPS ranges are needed instead of three because the GPS signals travel at the speed of light, c. A clock error, δt, of only one microsecond would results in a three hundred meter range error. Thus the GPS receiver clock error needs to be estimated to achieve useful position estimates. Due to the large uncertainty in range, the GPS measurements are referred to as pseudoranges to indicate the values are not absolute. Each active GPS satellite has a uniquely modulated carrier signal. The modulated signal comes in the form of a repeating sequence called a pseudorandom noise (PRN). The pseudorandom noise codes are known by the GPS reciever, which will compare the received signal to a list of internal pseudorandom noise codes, allowing the GPS receiver to determine which satellite the signal came from. The signal also has a navigation message modulated on top of the PRN, which contains a time of broadcast and the position of the broadcasting GPS satellite. By differencing the time of broadcast and received time and then multiplying by the speed of light, pseudorange can be estimated. When more than four signals are received, the position and clock timing uncertainty can be further decreased with a least squares approach.

The carrier phase measurement is an estimate of the phase of the received GPS signal, which allows for a precise range estimate because the wavelength of the GPS signals are only 19.0 cm for L1 and 24.4 cm for L2. Knowing the phase of an incoming signal accurately provides a source of centimeter or millimeter range measurements, sometimes called phaserange measurements. The Novatel receivers measure Accumulated Doppler Range (ADR) phaserange measurements. The primary limitation to this measurement type is the number of cycles between the transmitting GPS satellite and the Novatel receiver cannot be directly observed, so the measurements can be off by an integer multiple of wavelengths. The phaserange measurements are often expressed in an estimated number of cycles, hz, of the carrier frequency between the transmitter and the receiver or in distance units if estimated number of cycles are multiplied by the carrier wavelength. When multiple carrier frequencies are observed simultaneously the receiver can mathematically combine the two frequencies to remove the 1st order ionosphere time delay effects, which allow for further refined position estimates.

For precision orbit determination, the raw pseudorange and phase measurements are used, with the single point positions solutions only being used as an initial guess for the spacecraft state vector. During precision orbit determination the estimated parameters list will be expanded to include additional terms for time biases, measurement biases, spacecraft orientation parameters, and empirical force with once-per-rev and twice-per-rev terms. These parameters can be estimated due to the abundance of GPS measurements and their observability from the GPS measurements.

2.2.2 Intersatellite Laser Ranging Measurements

To supplement the GPS measurements, laser ranging measurements will be taken when the two CubeSats are in close proximity. Due the satellites moving at approximately $7.6 km/s$ in the intrack direction, the intrack positioning tends to have the largest uncertainty. Laser ranging measurements provide a measurement sensitive to intrack relative position differences between the two satellites, which can be used to constrain the relative intrack positioning. The relative positioning is not explicitly addressed in the this paper, but the laser ranging effects on the absolute positioning are examined.

2.2.3 Groundbased Satellite Laser Ranging

In addition to precision orbit determination performed using the on board GPS receiver and optical laser ranging measurements, an independent orbit determination will be conducted using ground

based satellite laser ranging (SLR) measurements which will be provided courtesy of the NRL and the ILRS. The RANGE satellites have reflective exteriors, suitable for laser ranging measurements. These ground based satellite measurements provide an opportunity to validate the accuracy of the orbit solutions which use the CubeSat measurements with the orbit solutions from the ground based SLR measurements. The SLR measurements are accurate to the millimeter level [9], which often allows for orbit solutions below the meter level. An agreement of two independent orbit determination methods using different measurement types would validate the orbit determination solution from the on board measurements. To the authors knowledge cross validation of precision orbit determination solutions with SLR measurements has not been done before for CubeSats. Additionally, during times of SLR measurements the combined data sets may be able to be combined for an even further refined orbit solution.

2.3 Software Simulations

Software simulations of expected on orbit GPS and laser ranging measurements were generated using the orbit determination software package called the Orbit Determination Tool Kit (ODTK). ODTK was used to investigate theoretically achievable orbit determination solutions for the following test cases: regular operations, the addition of laser ranging measurements and increased GPS measurement logging frequency. The effects of antenna misalignment and performing orbit determination without the CSAC were also investigated. The orbit uncertainties are discussed in the section 3.1. The state and measurement uncertainties used in the simulations come from the component spec sheets of the RANGE CubeSats hardware. The measurement processing scheme and force models are described in the following sections.

2.3.1 ODTK Processing Scheme

The orbit determination processing scheme used in ODTK is to take in an initial state estimate using the Novatel's bestxyz log, which is the single point positioning solution of the CubeSat while in orbit. The accuracy of the single point positioning is discussed further in section 2.4. The single point position estimate also includes a velocity estimate and uncertainties to populate the covariance. If the initial state is not accurate, then a batch least squares can be run using either multiple single point positioning measurements or by directly using the GPS pseduorange and phase measurements to find a more refined initial state and covariance. Once a refined initial state is determined, it is passed into an extended Kalman filter for precision orbit determination using the GPS pseudorange and phase measurements from the rangecmp2 log. After running the extended Kalman filter, a smoother is used to back propagate the state to find the best estimate of the CubeSat's state vector and covariance [10, 11].

2.3.2 Force Models

A moderate fidelity force model was chosen when investigating orbit determination accuracies. The forces are shown in figure 4. The choice of a moderate fidelity force model was made to capture the bulk effects of the real dynamics while still keeping the number of errors sources and software run time manageable. For processing of real measurements, a higher force fidelity model will be used with more specific drag, solar radiation pressure and reflectivity coefficients measured for the RANGE CubeSats, and potentially a more specific drag model.

During the orbit propagation, the attitude of the CubeSats are assumed to be in the default high drag orientation. The CubeSats will have the 1.5U face of the CubeSat facing along the in track direction with the GPS antenna oriented in the zenith direction. For real measurement processing the satellite ballistic coefficient can either be estimated or an attitude file will be can used.

Satellite Force Model	
Force	Value
Gravity	
μ_{Earth}	$3.986004415e^{14}\ m^3\ sec^{-2}$
Degree	21
Order	21
Solid Tides	true
General Relativity	true
Variational Equations	
Degree	2
Order	0
Third Bodies	
μ_{Moon}	$4.902794e^{12}\ m^3\ sec^{-2}$
μ_{Sun}	$1.32712438e^{20}\ m^3\ sec^{-2}$
Drag	
Atmosphere Model	Jacchia-Bowman 2008
Model	Spherical
C_D	2
Cross Sectional Area	$0.045\ m^2$
Solar Radiation Pressure	
Model	Spherical
C_r	1
Cross Sectional Area	$0.045\ m^2$
Reflection Model	Perfect Absorption
Eclipsing Bodies	
Earth	true
Moon	true
Earth Radiation	
Albedo	true
C_k	1
Cross Sectional Area	$0.045\ m^2$

Figure 4: Forces used for orbit propagation, simulated measurements and measurement processing

The initial orbit state and measurement uncertainties are listed in figure 5. The initial state position and velocity uncertainties originate from the expected accuracy of the single point positioning uncertainties as listed in the Novatel users OEM6 Family User manual [6], with a slightly larger initial uncertainty used for the in track direction. The orbit determination process is not very sensitive to these initial covariances as long as the initial orbit estimate is in the neighborhood of the real state. The clock phase uncertainty when using the CSAC assumes a conservative 1e-11 second uncertainty. The clock phase uncertainty without using the CSAC and the GPS measurement uncertainties also come from the Novatel Family OEM6 User manual. The simulated GPS measurements in ODTK do not use the two different frequencies uncertainties for L1 and L2 directly, rather the two frequencies are replaced by a L1 L2 dual frequency measurement which eliminates the first order ionospheric time delay effects. The GPS orbits come from the final IGS orbit solutions contained in the sp3 files on GPS week 1873 [12]. The position uncertainties are assumed to be 5 mm for all of the satellites. The velocity uncertainties and GPS clock uncertainties are the default values in ODTK. Individual GPS position uncertainties and clock biases can be estimated during measurement processing of real data.

Uncertainty Estimates	
Uncertainty	Value
Orbit	
σ_{Radial}	$1.5\ m$
$\sigma_{InTrack}$	$3\ m$
$\sigma_{CrossTrack}$	$1.5\ m$
$\sigma_{Radial,dot}$	$3e^{-2}\ m\ sec^{-1}$
$\sigma_{InTrack,dot}$	$3e^{-2}\ m\ sec^{-1}$
$\sigma_{CrossTrack,dot}$	$3e^{-2}\ m\ sec^{-1}$
Clock	
$\sigma_{phase,CSAC}$	$1e^{-11}\ sec$
$\sigma_{phase,NoCSAC}$	$2e^{-8}\ sec$
$\sigma_{frequency}$	$1e^{-12}$
L1	
$\sigma_{Pseudorange}$	$4e^{-2}\ m$
σ_{Phase}	$5e^{-4}\ m$
L2	
$\sigma_{Pseudorange}$	$8e^{-2}\ m$
σ_{Phase}	$5e^{-4}\ m$
L1 L2 Dual Frequency	
$\sigma_{Pseudorange}$	$8e^{-2}\ m$
σ_{Phase}	$1e^{-3}\ m$
GPS Orbit	
σ_{Radial}	$5e^{-4}\ m$
$\sigma_{InTrack}$	$5e^{-4}\ m$
$\sigma_{CrossTrack}$	$5e^{-4}\ m$
$\sigma_{Radial,dot}$	$1e^{-3}\ m\ sec^{-1}$
$\sigma_{InTrack,dot}$	$1e^{-3}\ m\ sec^{-1}$
$\sigma_{CrossTrack,dot}$	$1e^{-3}\ m\ sec^{-1}$
GPS Clock	
σ_{phase}	$3e^{-9}\ sec$
$\sigma_{frequency}$	$3.5e^{-14}$

Figure 5: State and measurement uncertainties

2.4 Hardware Validation

To ensure the accuracy of the Novatel receiver, GPS signals were gathered with the flight hardware. The first testing of the Novatel receivers was done outside to confirm their functionality. The Novatels were connected to the GPS antennas and then taken outside to a local field which was partially obscured by surrounding buildings and trees. From a cold start, the Novatels were generally able to acquire at least 4 GPS signals within a few minutes. Over the next few minutes, the Novatels were able to acquire signal locks for all of the satellites within the field of view not blocked by buildings or trees. Occasionally, the receivers were not able to get signal locks and had to be restarted. After restart, the receivers were usually able to pick up the GPS signals within minutes. The Novatel receivers were frequently able to achieve single point position accuracies of 2 meters in the horizontal directions and less than 5 meters in the vertical direction. After initial confirmation that the hardware performed as expected, a more rigorous validation of the Novatel receivers was performed with hardware in the loop testing.

The hardware in the loop simulation involved connecting the Novatel receivers to the NavX NCS GPS signal generator. The NavX NCS GPS signal generator can generate hardware radio frequency (RF) signals for the GPS constellation. The NCS GPS signal generator takes in a user position and then generates the RF signals the user would experience from the GPS constellations in the L1 and L2 frequencies. The GPS generator can also simulate Keplerian orbits, however there are no force models being used other than treating the Earth as a point mass [13].

The port where the GPS antenna is normally connected on the Novatel boards was instead connected to a 50 Ohm coaxial cable leading to the RF output of the GPS signal generator. The GPS signal generator was set to physically generate RF signals for a 500 km sun synchronous orbit,

with the user position provided from a propagated satellite in ODTK. To maintain consistency between different data collections, the GPS simulator was set to generate GPS signals starting at the same epoch. An interesting situation arose where the Novatel receivers initially had their internal clocks near the current date which was many months off of the simulated time. After a few minutes of waiting for the internal clocks to update and not acquiring signal locks, the Novatels were manually commanded to reset their internal clocks. Once being reset, the receiver accepted the incoming signals from the GPS simulator and were able to get signal locks for the simulated time frame. Usually within minutes the single point positioning solution was able to match the simulated position within orbit, usually reporting 1σ position uncertainties of less than 10 meters in each of the X,Y and Z components. The ability for the single point positioning solution to match the simulated orbit position confirmed the removal of the velocity and altitude restrictions by the manufacturer.

Two 12 hour data collections were performed with the GPS simulator, one without the CSAC and one with the CSAC. During each data collection the log bestxyz and rangecmp2 were recorded every 1 second [14]. The bestxy log contains the single point positioning solution and the 1σ uncertainties of the x, y and z components in the Earth fixed frame. The rangecmp2 log contains the pseudorange, phase and doppler shift of the L1 and L2 frequencies, as well as the associated 1σ uncertainty for each measurement. The bestxyz log is available in ASCII format, while the rangecmp2 log is in a compressed format to save storage space and needs to be decoded on the ground to access the GPS measurements. The decoding scheme is located on the Novatel support page [15]. Once the rangecmp2 logs were decoded, the logs are filtered to ignore times when the Novatel did not have an accurate signal lock. The times of observations which did not have a clock steering of "FINESTERRING" were ignored. Additionally, the logs were filtered to exclude measurements with self reported 1σ uncertainties greater than 4.5 cm for the pseduoranges and 0.0221 hz for the carrier phase.

After extracting and filtering the rangecmp2 logs, the measurement biases and uncertainties of the Novatel receiver in the hardware in the loop simulation were characterized. The measurements from the rangecmp2 log were differenced with the GPS measurements reported by the GPS signal generator. The GPS measurements generated by the GPS signal generator are reported in the form of RINEX logs. According to the NavX NCS signal generator data sheet, the generated signals will match the reported RINEX logs to within 2 mm RMS for the pseudoranges [16]. The RINEX logs are taken to be the "truth" measurements. The rangecmp2 log measurements generated by the Novatel are the "observed" measurements. Section 3.2 shows the differenced measurements without the CSAC and 3.3 shows the differenced measurements with the CSAC.

3 Results

3.1 Simulated Results

The following sections demonstrate theoretically observable orbit determination position accuracies for different operational modes of the RANGE CubeSats. The CubeSats have enough on-board storage to collect GPS measurements approximately two times per minute between data downlinks. To allow room for other data collection and margin, the orbit determination analysis is performed assuming the Novatel receivers are set to log once per minute during regular operations. During times of near proximity operations, the intersatellite laser ranging measurements and GPS measurements may be logged as frequently as once per second. The estimated orbit determination position results during these operational modes are presented. Additionally, effects on the orbit determination solution from potential sources of error such as GPS antenna misdirection and effects without the CSAC are examined. Other sources of error such as mismodeled forces and measurement biases are discussed.

Simulated measurements for these different operation modes are generated inside of ODTK with the uncertainties and force models listed in the section 2.2. For comparison purposes, the measurements are assumed to have no biases and to have only a Gaussian white noise uncertainty. Thus allowing for a theoretical limit for a orbit determination solution using the RANGE hardware. During orbit determination with real measurement data, a time varying bias for the receiver clock phase and frequency and measurement biases will be estimated. If force models and measurement biases can be estimated with sufficient precision, the orbit determination solution with real measurement should approach the theoretical orbit determination solutions presented here.

3.1.1 Regular Operations

During regular operations, the CubeSats are set to log GPS pseudorange and phase in the L1 and L2 frequencies once per minute. Figure 6 shows the expected radial, in track and cross track 3σ uncertainties. The measurements collected assume the CubeSat is oriented in the default high drag configuration, allowing the GPS antenna to face directly zenith. Any GPS satellites within 90 degrees of zenith are considered due to the hemispherical shape of the GPS antenna. The 3σ positions indicates a 99.73% level of confidence along the given radial, intrack or crosstrack direction. The radial uncertain is consistently the largest uncertainty oscillating around 9 cm. The intrack uncertainty oscillates around 5 cm and the crosstrack uncertainty oscilates around 7 cm. These oscillations in the orbit uncertainties are dependent on the current number of satellites being observed and their geometric spacing relative to the CubeSat receiver known as the dilution of precision.

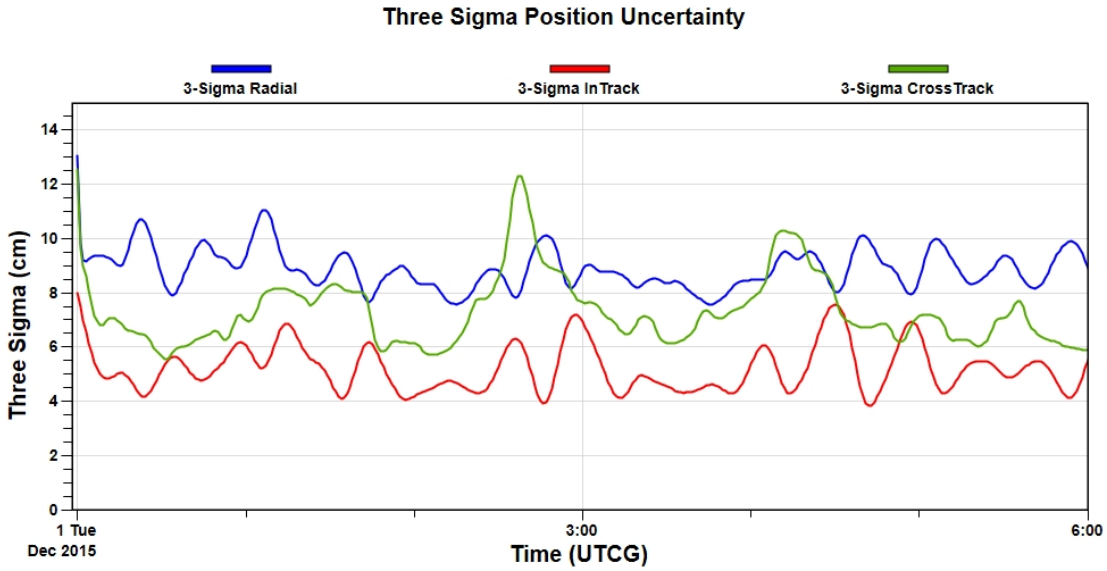

Figure 6: Simulated results using 1 minute measurements and assuming a hemispherical zenith pointing antenna

3.1.2 Laser Ranging

During time periods when the CubeSats are within a few kilometers of each other, the laser ranging system can be utilized to send accurately timed pulses between CubeSats to gather ranging measurements. Inside ODTK, these measurements are simulated simply as a satellite based range measurements with an associated ranging uncertainty and an optional measurement bias. The laser ranging measurements are assumed to be gathered every minute with the 50 mm ranging uncertainty used for multi-pulse signals. The simulated satellites are separated by 0.001 degrees or true anomaly, which corresponds to a 120 m absolute position offset. Both CubeSats are assumed to be in regular operation mode and processing regular 1 minute GPS measurements with the addition laser ranging measurements of one CubeSat observing the other. The results displayed here are for the absolute positions orbit uncertainties.

Interestingly, the the shape of the orbit uncertainties appear to exhibit a peak in intrack uncertainty around the 3rd hour, with slightly lower orbit uncertainties surrounding the peak in intrack uncertainty as shown in figure 7. When compared to orbit uncertainties during regular operations the absolute positioning is not considerably improved by the laser ranging measurements with a 50 mm uncertainty, however the laser ranging measurement did change offer some change in the shape of the covariance ellipsoid over time. The marginal to lack of absolute positioning improvement is likely due to the orbit position solution already being on the order of a to within 10 centimeters in all 3 radial, intrack and crosstrack directions. The incorporation of more measurement biases and estimated parameters could potentially be better estimated with the addition of laser ranging measurements, but that is not investigated here. The effects of increasing the measurement fre-

quency of the laser ranging to 1 second was also investigated, but the resulting graph was nearly indistinguishable from figure 7, and thus not shown here.

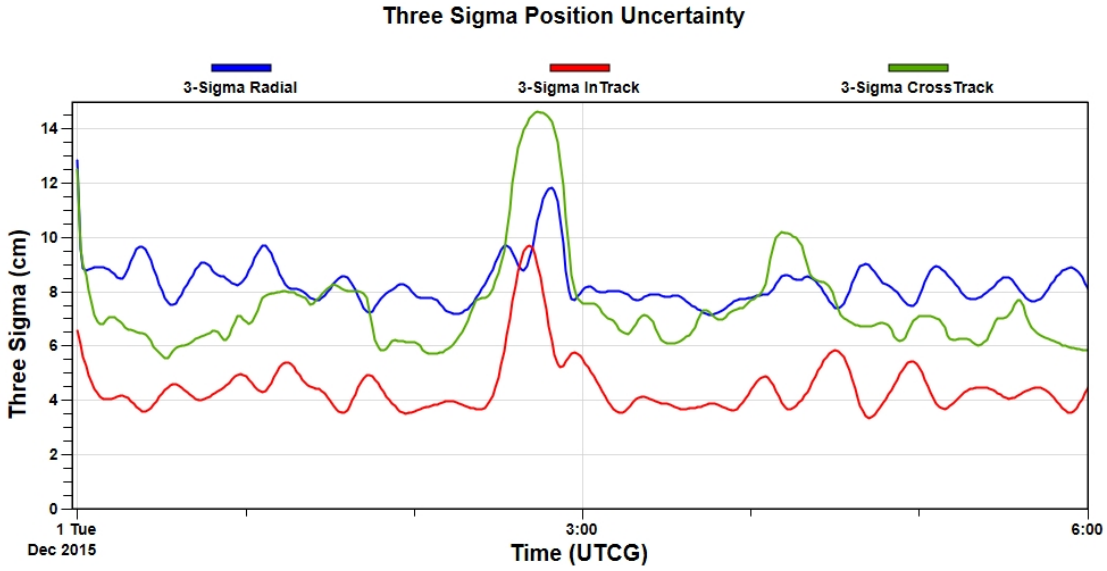

Figure 7: Simulated results using 1 minute measurements and assuming a hemispherical zenith pointing antenna. Considering 1 minute laser ranging measurements with a 50 millimeter ranging uncertainty.

3.1.3 Increased Observation Frequency

During times of interest, when there is adequate on-board storage, the Novatel receiver will be commanded to log GPS measurements every 1 second. One such time period, will being during SLR ground based measurements used to validate the orbit solution. Figure 8 shows the position uncertainties when processing simulated GPS data logged every 1 second. The radial 3σ position uncertainty fluctuates around 2 centimeters, while the cross track 3σ uncertainty fluctuates between 1 and 2 cm and the intrack 3σ uncertainty stays about 1 centimeter. Increasing measurement frequency shows a significant improvement on the orbit determination accuracy. However, long periods of 1 second observations are not sustainable on a CubeSat platform due to data storage restrictions. The 1 second logging will need to be limited to specific short time frames of interest.

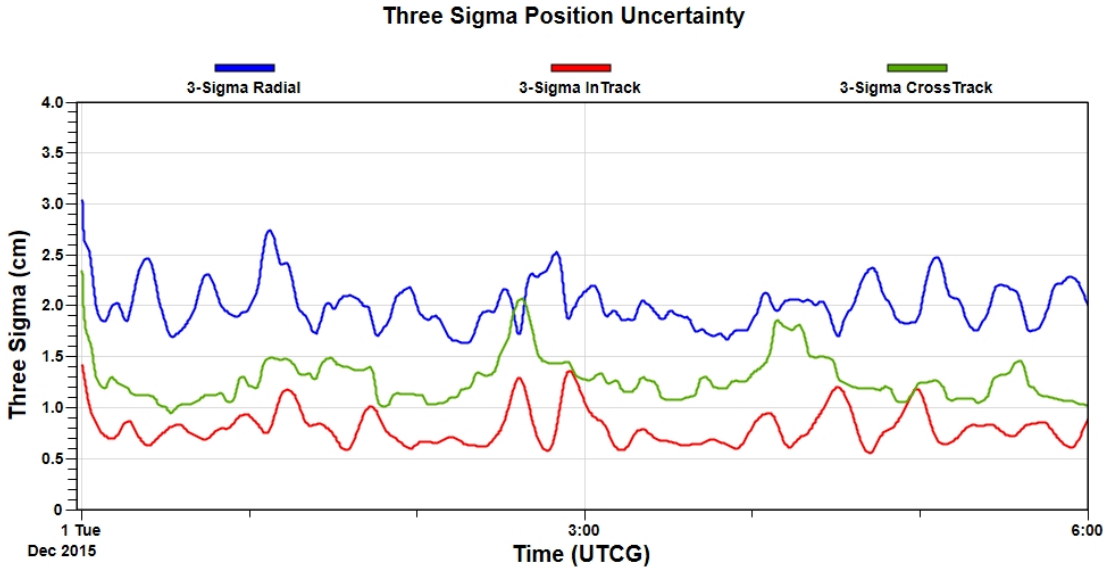

Figure 8: Simulated results using both 1 second GPS measurements

3.1.4 Error Modeling

3.1.5 Accounting for Misdirection of the Antenna

The previous figures assumed nearly ideal antenna alignment, with the GPS antenna having it's main lobe gain pointed directly in the zenith. However, the CubeSats will be changing attitude to perform differential drag maneuvers. In nominal low drag mode, the GPS antenna will be facing towards the velocity direction of the CubeSat. In this orientation, a large portion of the the antennas field of view is blocked by the Earth. Thus allowing for only a portion of the GPS satellites to be observed. Figure 9 shows the expected 3σ uncertainties when the GPS antenna is oriented 90 degrees from zenith towards the velocity direction, either due to being in low drag orientation, or an unintended misalignment of the antenna. Note, the axes have been rescaled to 25 cm. In this orientation, all three components uncertainties have grown when compared to 6. All three components oscillate between 10 and 20 cm for the 3σ uncertainties, as less measurements are being taken in and the orbit solution becomes more reliant on the number of GPS satellites in the antenna's field of view. The orbit uncertainties are approximately doubled, which indicates the CubeSats will need to be in high drag mode to achieve single digit centimeter level 3σ positioning accuracies.

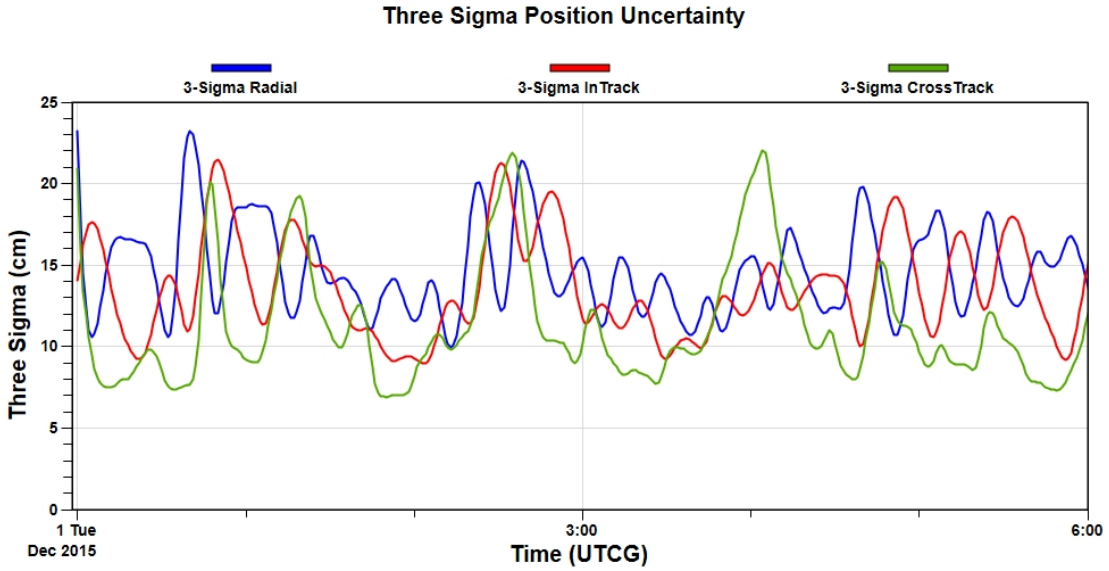

Figure 9: Simulated results using 1 minute measurements and assuming an antenna aligned with the velocity direction

3.1.6 Effects without the CSAC

In the event of a CSAC failure or the CSAC does not improve the Novatel clock uncertainty, the Novatel default clock uncertainty of $2e^{-8}$ seconds is used for measurement processing. Figure 10 shows the processed GPS measurements without the use of the CSAC. The theoretically achievable position uncertainties remain unaffected after the first few minutes of observations. However, this results makes the assumption that there is no time bias or that the time bias can be completely eliminated, which is likely not be a completely valid assumption. The CSAC allows for the time bias to be stabilized and therefore likely to be more easily estimated, as briefly discussed in section 3.3.

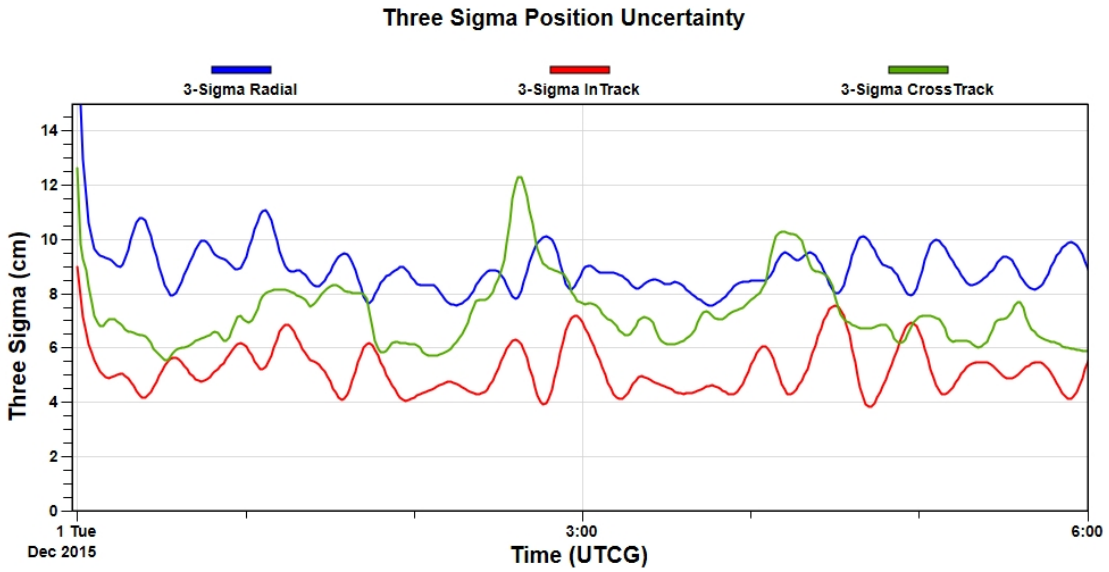

Figure 10: Simulated results using 1 minute measurements and assuming a hemispherical zenith pointing antenna. The CSAC time uncertainty is not used, instead the $2e^{-8}sec$ Novatel time uncertainty is used.

3.1.7 Mismodeled Forces and Measurement Biases

As shown the above, the CubeSat hardware with the orbit processing scheme is capable of producing position solutions down to the centimeter level. However, to achieve such accurate solutions, the force models used must be modeled and matched very accurately to the forces the CubeSats will experience on orbit. Here lies the one of the largest sources of error for orbit determination. Mismodeling the dynamics such as Earth's gravity field, solid tides, ocean tides, atmospheric drag and solar radiation pressure can all produce errors on the centimeters level [17]. To reduce the uncertainty in the RANGE spacecraft physical properties, the mass is known to within grams, the spectral reflectance has been measured, and the physical dimensions are known to the millimeter level, thus the spacecraft properties mismodeling will likely have much smaller contribution to orbit uncertainty than the force model mismodeling. To account for force model mismodeling, the use of secular and periodic empirical force may be employed to absorbs some of the force model uncertainty.

Another large source of error that was initially ignored in these simulations are measurement and time biases. Theoretically these biases can be estimated and removed, however, if they are not able to be estimated very accurately the orbit solution uncertainty will grow. The hardware validation results presented in the following sections characterizes the types of time bias and measurement uncertainties expected with the RANGE hardware. These biases estimates can serve as an initial estimate for the biases which will arise in real data.

3.2 Hardware Validation Without the CSAC

Figure 11 shows total position errors between single point positioning from the bestxyz log and the position used for the GPS signal generator. The bestxyz logs were filtered to remove any times which did not use "FINESTERRING" and to remove any times with self reported 1σ position measurement uncertainties of greater than 20 m in any x,y or z component. Looking at the figure, 78% of the of bestxyz logs were within 10 m of the true position, but frequently the position errors would grow into the 10s of meters. By examining the bestxyz logs an initial orbit state could likely be selected to be within 10 meters of the true position. Even if the initial state vector chosen was not within 10 meters of the true position, all of the states were within 100 meters of the true position, which is likely a good enough initial state for the precision orbit determination process.

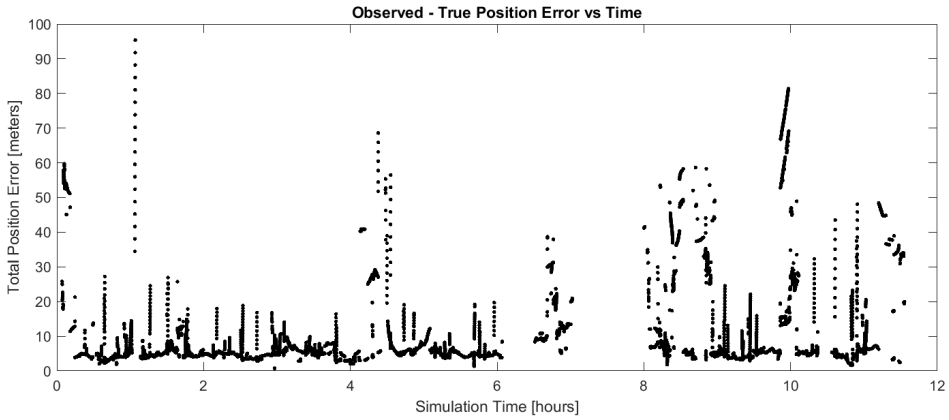

Figure 11: Observed - truth for the L1 pseudorange measurements without using the CSAC

Figure 12 shows the differences between the "truth" and "observed" L1 pseudorange measurements without using the CSAC from the hardware in the loop orbit simulation.

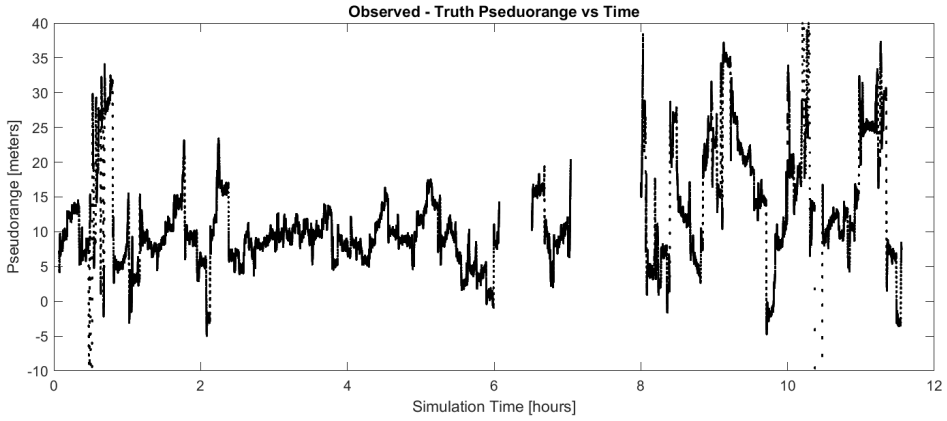

Figure 12: Observed - truth total position errors without using the CSAC

Initially the L1 pseduorange differences appear to be on the order of meters, with a mean of 11.1 cm $\pm$ 9.1 cm for the 1σ uncertainty, however the majority of this error is likely caused by a time bias. This become apparent when looking at the pseudorange measurements for each observation time. Figure 13 shows a sample of the pseduorange measurements over a 1 minute time scale.

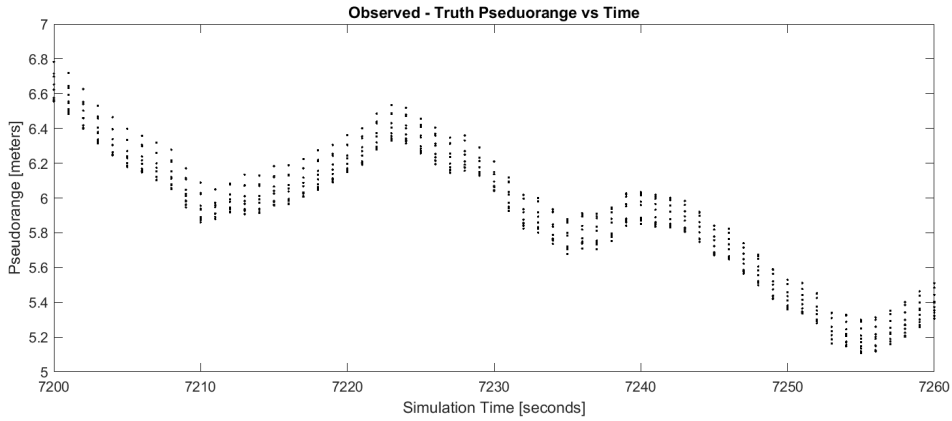

Figure 13: Observed - truth for the L1 pseudorange measurements over a 1 minute time scale

The clustering of pseudorange measurements can be more readily seen when looking at each measurement time. The mean pseudorange error changes notably between each measurement. The carrier phase measurements mimics this behavior, indicative of a time bias. By taking the mean pseudorange error at each measurement time and then dividing by the speed of light, a time bias at measurement time can be approximated. Figure 14 displays an approximate time bias of the Novatel from the hardware in the loop simulation.

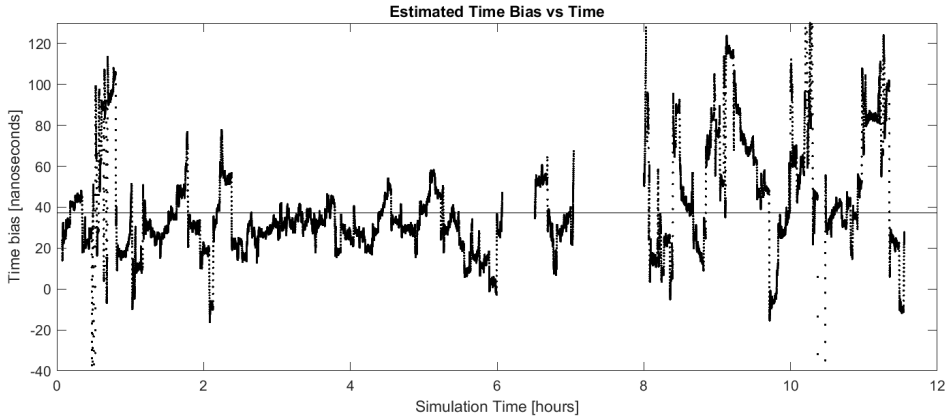

Figure 14: An estimated time bias for each measurement, by dividing the mean pseudorange error by the speed of light for each measurement. The mean time bias is plotted as a horizontal line.

The approximate time bias is a combination of any time delay during the signal generation process, the RF signal delay in the coxial cable and the Novatel's clock instability. As well as any actual pseudorange bias that gets absorbed into the approximate time bias. The Novatel OEM6 Family User Manual quotes the timing bias uncertainty to be 20 nanoseconds RMS [6]. From the hardware in the loop simulation, the mean time bias is 37.2 nanoseconds with a 30.4 nanosecond standard deviation about the mean. During the orbit determination process with real measurements, a time variable measurement time bias will need to be estimated, allowing the time bias effects on the measurements to be mostly removed. Figure 15 and 16 show the standard deviations of the L1 pseduorange and phaserange within each measurement time, after subtracting off the mean pseudorange or phaserange error. Note the standard deviation here is between the differences in the errors of multiple GPS satellites, and not relative to each individual satellite. Under the assumption that each GPS satellite have the same time biases, which is true for the hardware in the loop simulation, and the total receiver time bias is not very large, the standard deviation between the measurements of different satellites should be quite similar to the standard deviation of measurements to an individual satellite.

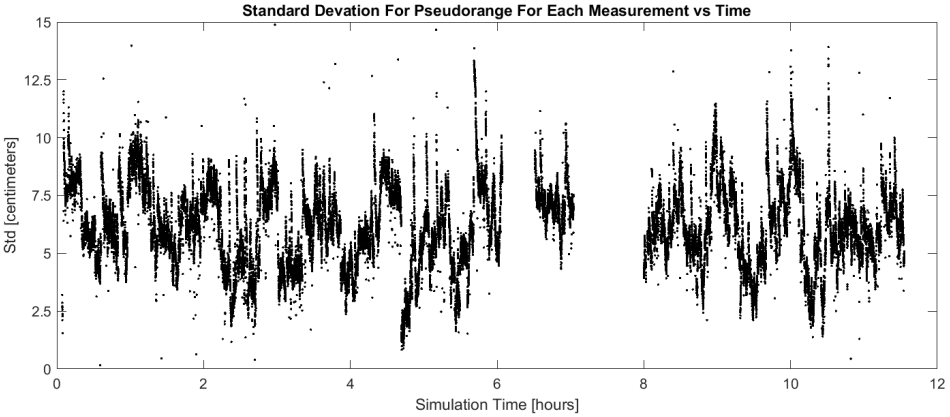

Figure 15: The standard deviation between the observed - truth L1 pseduoranges using all of the observed satellites at each measurement time.

The average standard deviation for L1 pseudoranges errors is 6.2 cm, which is 1.5 times greater than the value of 4 cm RMS quoted for the just the Novatel's expected accuracy [6]. The L1 pseudorange data graphed was filtered to only include self reported 1σ uncertainties of 4.5 cm from the rangecmp2 log and ignore any outliers with large uncertainties.

The L1 phase range standard deviation shown in figure 16 has a mean value of 4.4 mm. The mean value is brought up by a few decimeter level outliers not shown within the figure. Excluding

these outliers, the mean value of the L1 phase range standard deviation is 2.0 mm, which is 4 times higher than the expected 0.5 mm RMS for just the Novatel [6]. The 2.0 mm mean value may be approaching the limitation of GPS signal generator's ability to produce the correct signal phase [16]. All of the data displayed in the figure has a self reported 1σ uncertainty of 2.4 mm or less from the rangecmp2 log.

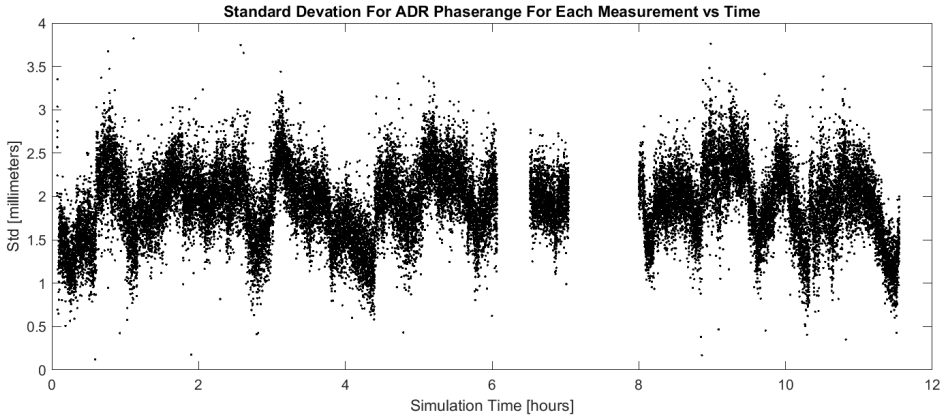

Figure 16: The standard deviation between the observed - truth L1 ADR phaserange using all of the observed satellites at each measurement time.

When the Novatel receives both the L1 and L2 frequencies, the signals are combined to create a dual frequency base pseudorange and phase measurement which is free from the first order ionospheric time delay effects. Thus the L1 and L2 frequencies both experience the same receiver time bias effect and will have similar plots, because of this separate plots are not presented here.

3.3 Hardware Validation With the CSAC

Figure 17 shows total position errors between single point positioning from the bestxyz log and the position used for the GPS signal generator when using the CSAC. The bestxyz logs were filtered to remove any time not using "FINESTERRING" and to ensure no 1σ measurement uncertainties were greater than 20 m in any position component. Looking at the figure, it is immediately clear that there are less data points when the CSAC was used, and of the points only 55% of the data points were within 10 meters of the true solution as compared to 78% when the CSAC was not used. Still any bestxyz log selected would put the observed orbit with 100 meters of the true orbit, which is likely a good enough initial guess for precision orbit determination. It is work noting that the single point positioning is estimating and handling a large growing time bias which will be discussed in the following sections.

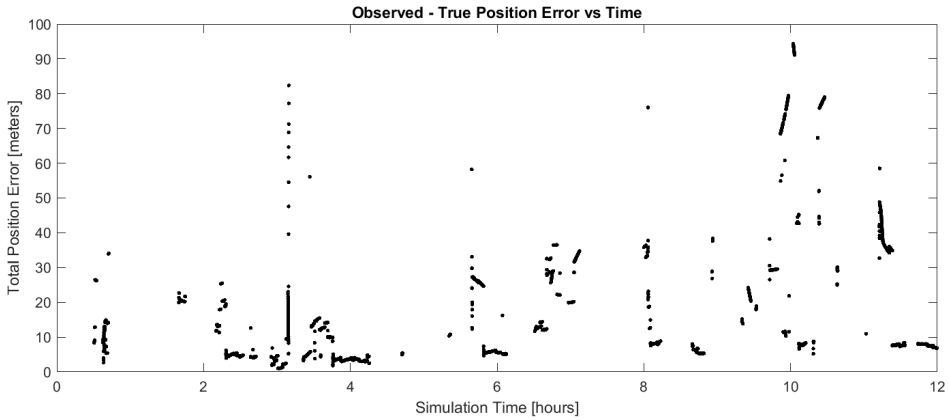

Figure 17: Observed - truth total position error when using the CSAC

When comparing the "observed" measurements to the "truth" while using the CSAC, the measurements continually deviated in a near linear fashion. At each measurement update the pseudoranges were an additional 6.9 $\pm$ 0.1 m further away from the truth. Making the same assumptions as in the previous section, the time bias appears to be growing at a near constant 23.2 $\pm$ 0.20 nanoseconds/second. This indicates that the external oscillator is discipling the Novatel's internal clock and holding it steady, however, the length of the second is consistently 23.2 nanoseconds too short and not adjusted once the Novatel acquires a GPS signal lock. Figure 18 demonstrates the drift of the pseduorange error measurements over 12 hours.

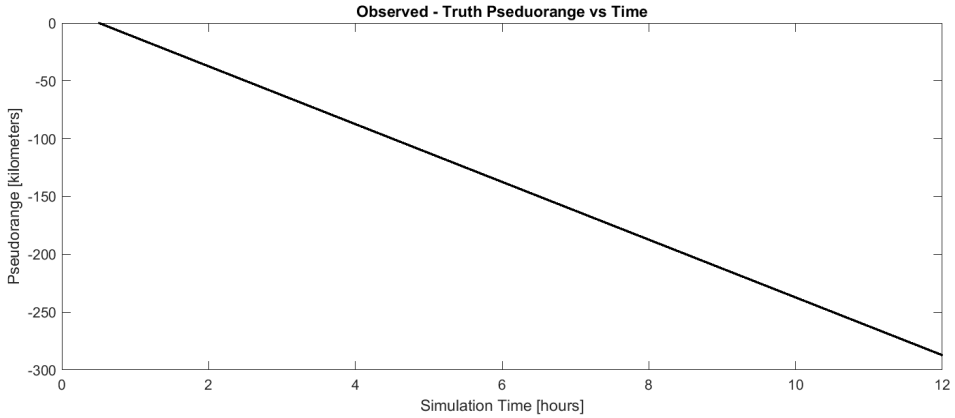

Figure 18: Observed - truth for the L1 pseudorange measurements with the CSAC. A consistent growing measurement bias of 6.9 meters/second is observed.

Instead of plotting the time bias as done previously, the time bias drift rate is plotted in figure 19. The figure shows the majority of the time bias drift rates packed closely along the 23.2 nanoseconds/second line. A slight correction to the time bias drift rate can be seen during the 3 hours after a GPS signal lock has been acquired by looking at the blue line representing the 30 minute moving average. The total correction over the first 3 hours is approximately 0.08 nanoseconds or 8e-11 seconds, which is similar to what might be expected when referencing figure 3 a) where the CSAC's stability transitions from an initial Allan Deviation of 8e-11 seconds at the first second to 1e-12 seconds after 10e4 seconds (2.78 hours). This indicates the Novatel and CSAC are working in pair to become more stable. The 0.20 nanoseconds/second 1σ uncertainty is likely not an indicator of the clock instability, rather it is likely a limitation of the time bias estimation. The L1 pseduoranges without the CSAC were shown to have an average 1σ standard deviation of 6.2 cm, which would correspond to a 0.21 nanosecond/second 1σ standard deviation when estimating the time bias.

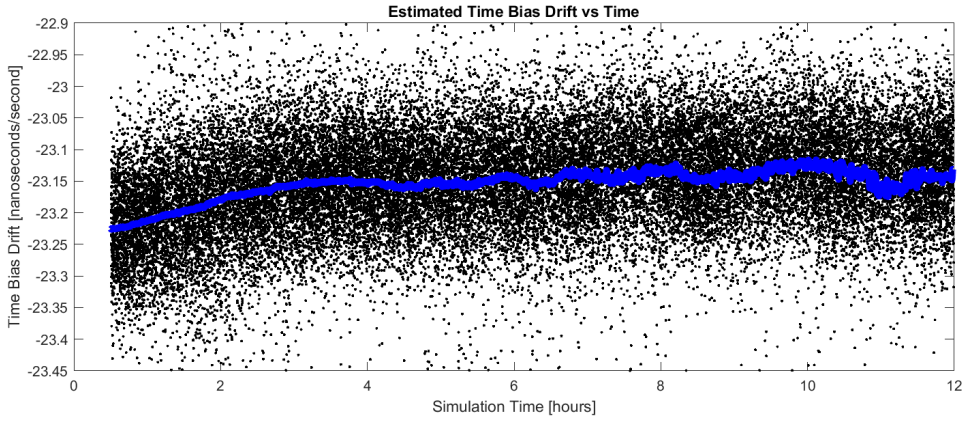

Figure 19: The estimated time bias drift rate, estimated by differencing the mean pseudorange error between measurements then dividing by the speed of light. The 30 minute moving average is plotted in blue.

The time bias drift with the CSAC is more stable than without, however, the total time bias is much larger. The constant additive time bias of 23.2 nanoseconds results in a range error of approximately 300 km over the 12 hour observation period. Due to the non-linear nature of orbital motion, simply differencing the observed and truth measurements results in measurement errors with large standard deviations as the intrack and radial position offsets grow. From inspection, the standard deviations also appear to be correlated with the 95 minute orbit period. However it is worth noting, in the first 15 minutes after a GPS signal lock, the initial L1 pseduorange standard deviations also have a mean of 6.2 cm, which is in agreement with the results without using the CSAC, as shown in figure 21. The ADR phaserange standard deviation also exhibits a similar trend, starting around 2 millimeters for the 1σ uncertainty, which is in agreement with the results without using the CSAC and then the measurement uncertainty rapidly grows. The plot is not shown here. For a more accurate estimate of the pseudorange and phase measurements uncertainties when using the CSAC, the time bias will need to be estimated and removed during the orbit determination process and not by directly differencing the measurements.

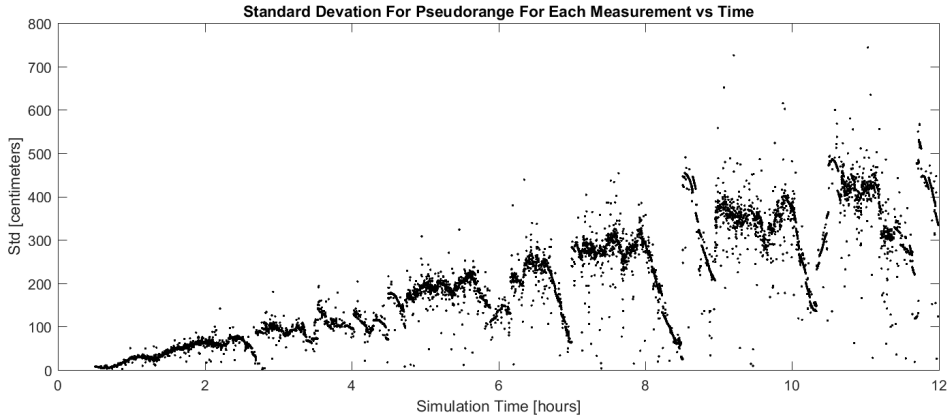

Figure 20: The standard deviation between the observed - truth L1 pseduoranges for all of the observed satellites at each time.

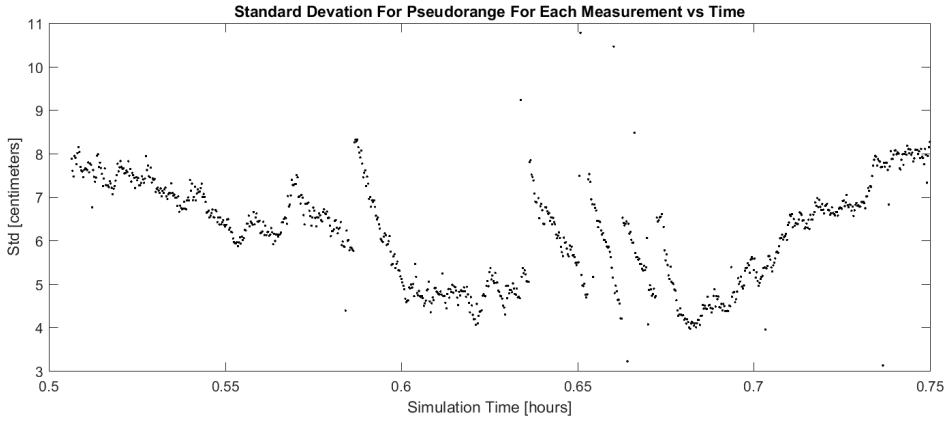

Figure 21: The standard deviation between the observed - truth L1 pseduoranges over the first 15 minutes of signal lock.

4 Conclusion

Simulated on orbit measurements using the hardware specs for the RANGE CubeSat have demonstrated the capability of post-processed orbit determination solutions to achieve single digit centimeter level 3σ uncertainties in the CubeSat's absolute positioning during periods of high frequency measurements. During regular operations when GPS measurements are collected once per minute the expected orbit determination 3σ accuracy should approach 10 cm or less for each of the radial, intrack and crosstrack components. Adding the laser ranging measurements between the two satellites with a 50 mm 1σ uncertainty, will likely not result in improved absolute positioning of the spacecraft assuming the 3σ orbit solutions are already known to within 10 cm for each of the radial, intrack and crosstrack components. The most significant improvement to the orbit determination solutions comes in the form of specific time periods when the RANGE CubeSats will be recording rangecmp2 logs every second. During these times the 3σ absolute position uncertainties for each of the direction components are 2.5 cm for the radial direction, 1 cm for the intrack direction and 1.5 cm for he crosstrack direction.

The investigated sources of error from a mission execution perspective included antenna misdirection and the Novatel GPS receiver without the CSAC. The antenna misdirection, had a notable degradation effect on the orbit determination solution, increasing the 3σ absolute position uncertainties to 10 to 20 cm, indicating that the most accurate orbit determination solutions will need to occur when the CubeSats are are in high drag mode, to allow the GPS antenna to gather more measurements. With the assumptions of no time biases made during the measurement simulations, the orbit uncertainty without the use of CSAC was not reduced. During measurement processing of real data, the CSAC will provide clock stability allowing for the time accuracy to likely be estimated more accurately, so that these theoretical values can be more closely achieved. The orbit determination solution accuracies presented here assume no measurement biases or force mismodeling, thus orbit uncertainties presented approach the theoretical limitations of the RANGE missions hardware.

As part of ensuring the CubeSats are capable of achieving these levels of orbit uncertainties, the Novatel receivers were tested in a hardware in the loop simulation with the NavX NCS GPS signal generator. The results from the hardware in the loop simulation indicate an approximate mean time bias of 37 nanoseconds with a 30 nanosecond 1σ standard deviation. The average standard deviation for the L1 pseudorange was 6.2 cm and 2 cm for the phaserange. These standard deviations are a mixture of the GPS signal generator's ability to generate the RF signals, the noise caused by the coaxial cable and the Novatel's ability to read the incoming RF signal. The time and pseduorange errors are both approximately 1.5 times the larger quoted in the Novatel OEM6 Family User Manual. The carrier phase error is 4 times larger than expected, however this larger discrepancy is likely due to GPS signal generators accuracy. The performance of the Novatel receiver has been shown to be in approximate agreement with the expected accuracy levels, assuming some of this discrepancy is from other aspects of the hardware in the loop simulation

and not completely from the Novatel. Results from the hardware in the loop tests with the CSAC, show improved clock stability when compared to the test without the CSAC. The improvement in the clock stability will likely help when estimating the clock bias. However, a constant drift of 23.2 nanoseconds/second was introduced when the CSAC and Novatel are used together.

The CubeSats are physically capable of achieving centimeter level position accuracy, however many considerations must be made to achieve this level of orbit accuracy such as matching force models precisely, matching Earth orientation parameters,estimating clock and measurement biases for the RANGE CubeSats and the time biases of the GPS satellites. Accounting for and eliminating all of these sources of error is a non-trivial task. Future work may include adding errors onto the simulated observations in ODTK and then estimating the receiver clock time and measurement biases. The GPS measurements from the hardware in the loop simulation cannot be be used directly, because the GPS signal generator interpolates the GPS ephemeris positions differently than ODTK resulting in many meters of pseduorange discrepancies. Instead, the errors from the hardware in the loop simulation could be added onto the simulated measurements in ODTK to estimate the biases of the Novatel receiver and their effect on the orbit solution accuracy. Additional considerations such as dealing with mismodeled forces by estimating empirical forces may also be explored to further quantify the RANGE mission's orbit determination capabilities. Future work for the RANGE mission may also include a comparison of orbit determination solutions between other orbit determination tools such as Gipsy X and MONTE.

References

[1] Bonin, G., Roth, N., Armitage, S., Newman, J., Risi, B., and Zee, R., "CanX-4 and CanX-5 Precision Formation Flight: Mission Accomplished!", Small Satellite Conference 2015, Jul 2015, https://digitalcommons.usu.edu/smallsat/2015/all2015/3/.

[2] Hwang, C., Tseng, T.-P., Lin, T., Fu, C., and Svehla, D., "Precise Orbit Determination for FORMOSAT-3/COSMIC and Gravity Application," *AGU Spring Meeting Abstracts*, Vol. 1, Apr 2005, p. 04.

[3] D, S. and M, R., "Kinematic and reduced-dynamic precise orbit determination of low earth orbiters," *Advances in Geosciences*, Vol. 1, Jun 2003.

[4] Wertz, J., Everett, D., and Puschell, J., *Space Mission Engineering: The New SMAD*, Hawthorne, CA: Microcosm Press, 2011.

[5] Bandyopadhyay, S., Foust, R., Subramanian, G. P., Chung, S.-J., and Hadaegh, F. Y., "Review of Formation Flying and Constellation Missions Using Nanosatellites," *Journal of Spacecraft and Rockets*, Vol. 53, No. 3, Mar 2016, pp. 567–578, https://doi.org/10.2514/1.A33291.

[6] Novatel, "OEM6 Family Installation and Operation User Manual Rev 12", pp. 145, https://www.novatel.com/assets/Documents/Manuals/om-20000128.pdf, Oct. 2016.

[7] Jackson Labs, "RSR CSAC GSPDO User Manual", http://www.jackson-labs.com/assets/uploads/main/RSR_CSAC_1.2.pdf, Jan. 2017.

[8] Voxtel Inc., "Eyesafe Laser Rangefinder (LRF) OEM Module", http://voxtel-inc.com/files/LRF-Product-Catalog.pdf, 2018.

[9] International Laser Ranging Service., https://ilrs.cddis.eosdis.nasa.gov/network/system_performance/index.html.

[10] Analytical Graphics Inc., ODTK A Technical Summary, http://help.agi.com/odtk/ODTK/pdf/mach10summary.pdf, Feb. 2009.

[11] Wright, J., "Orbit Determination Tool Kit Theory and Algorithms", http://help.agi.com/odtk/ODTK/pdf/MathSpec.pdf, Nov. 2013.

[12] International GNSS Service, ftp://ftp.igs.org/pub/product/1873/.

[13] IFEN GmbH, "NavX - NCS User Manual Version 1.10", 2015.

[14] Novatel, "OEM6 Family Firmware Reference Manual Rev 12", pp. 595-600, https://www.novatel.com/assets/Documents/Manuals/om-20000129.pdf, July 2017.

[15] Novatel, "APN-031: Decoding RANGECMP and RANGECMP2", https://www.novatel.com/assets/Documents/Bulletins/apn031.pdf, May 2017.

[16] IFEN GmbH, "NavX NCS Essential Simulators Data Letter", https://www.ifen.com/fileadmin/documents/pdf/NAVX-NCS-Essencial/NavX-NCS-ESL_Datasheet_Letter.pdf.

[17] Tapley, B. and Ries, J., Guidance, Navigation, and Control and Co-located Conferences, American Institute of Aeronautics and Astronautics, Aug 1997.